2010

A Simple Model to Predict Scalar Dispersion within a Successively Thinned Loblolly Pine Canopy

Steven L. Edburg
Washington State University, sledburg@gmail.com

Gene Allwine
Washington State University

Brian Lamb
Washington State University

David Stock
Washington State University

Harold Thistle
U.S. Department of Agriculture Forest Service

See next page for additional authors

Journal of Applied Meteorology and Climatology
Volume 49, Issue 9 (September 2010) pp. 1913-1926

A Simple Model to Predict Scalar Dispersion within a Successively Thinned Loblolly Pine Canopy

STEVEN L. EDBURG, GENE ALLWINE, BRIAN LAMB, AND DAVID STOCK

Washington State University, Pullman, Washington

HAROLD THISTLE

U.S. Department of Agriculture Forest Service, Morgantown, West Virginia

HOLLY PETERSON

Montana College of Mineral Science and Technology, Butte, Montana

BRIAN STROM

U.S. Department of Agriculture Forest Service, Pineville, Louisiana

(Manuscript received 30 June 2009, in final form 1 February 2010)

ABSTRACT

Bark beetles kill millions of acres of trees in the United States annually by using chemical signaling to attack host trees en masse. As an attempt to control infestations, forest managers use synthetic semiochemical sources to attract beetles to traps and/or repel beetles from high-value resources such as trees and stands. The purpose of this study was to develop a simple numerical technique that may be used by forest managers as a guide in the placement of synthetic semiochemicals. The authors used a one-dimensional, one-equation turbulence model (k–l_m) to drive a three-dimensional transport and dispersion model. Predictions were compared with observations from a unique tracer gas experiment conducted in a successively thinned loblolly pine canopy. Predictions of wind speed and turbulent kinetic energy compared well with observations. Scalar concentration was predicted well and trends of maximum observed concentration versus leaf area index were captured within 30 m of the release location. A hypothetical application of the numerical technique was conducted for a 12-day period to demonstrate the model's usefulness to forest managers.

1. Introduction

Bark beetles (Coleoptera: Curculionidae: Scolytinae), such as the mountain pine beetle (MPB; *Dendroctonus ponderosae*) and southern pine beetle (SPB; *D. frontalis*), kill millions of acres of trees in the United States annually (USDA Forest Service 2004). Aggressive species kill otherwise healthy trees and usually require host-tree death for reproduction. To accomplish this, they must attack en masse to overcome host-tree resistance, and then adequately space themselves to limit intraspecific competition. Both processes involve chemical signaling via insect- and host-produced semiochemicals, synthetic versions of which are deployed by forest managers to help meet various objectives. For example, synthetic attractants are used in beetle traps, and antiaggregation semiochemicals are used to protect trees and forested areas from attack by bark beetles.

Stand thinning (removing a subset of whole trees) has long been advocated to moderate tree losses to bark beetles, and it is an important component of programs designed to improve pine forest health in the Southeast and much of the United States (Nowak et al. 2008). However, mechanisms through which thinning affects forest losses to bark beetles are unclear, as are explanations for the inconsistencies observed with the application of synthetic semiochemicals for management of these insects. The interaction between forest stand density and chemical signaling by insects is a cornerstone of forest health and its policies, but has received limited research attention. More

Corresponding author address: Steve Edburg, Washington State University, P.O. Box 642910, Pullman, WA 99164-2910.
E-mail: sledburg@gmail.com

DOI: 10.1175/2010JAMC2339.1

specifically, forest managers lack quantitative information on semiochemical transport and dispersion within forest canopies. This knowledge could help guide deployment strategies of synthetic semiochemicals through knowledge about the source strength and placement of traps or semiochemical packets in sparse or dense forest canopies.

Semiochemical (or scalar) transport and dispersion within plant canopies is controlled by turbulence. Turbulence within and above plant canopies has been extensively studied since the late 1960s (Allen 1968). Forest canopy turbulence studies have been conducted in both dense (Baldocchi and Meyers 1988) and sparse (Baldocchi and Hutchinson 1987) canopies. The so-called family portrait of canopy turbulence statistics shown in Raupach et al. (1996), and reprinted in the review by Finnigan (2000), shows typical statistical characteristics of plant canopy flows that were developed with data from wheat to forest canopies. Turbulence statistics normalized by the friction velocity at the top of the canopy collapse, with few exceptions, to universal vertical profiles (Finnigan 2000). Characteristics of the normalized data include an inflection point in the mean wind speed near the canopy height ($z = h$), maximum shear near the canopy top, a constant stress layer above the canopy, strong momentum flux within the canopy, and high velocity variances within the canopy.

Few studies have been conducted to examine the effects of thinning on turbulence. Those that have suggest that thinning a canopy can affect its horizontal homogeneity. Individual trees create wakes where turbulence is mechanically produced and dissipated. Gaps between trees create differences in solar heating between the ground and vegetation surfaces (Lee 2000). Green et al. (1995) measured turbulent statistics with three component propeller anemometers in three stands of Sitka spruce with stem densities of 625, 278, and 156 trees per hectare, and leaf area index (LAI) of 3.20, 1.51, and 0.82 $m^2\ m^{-2}$. Because of stall speed concerns, only periods with wind speeds greater than 2 $m\ s^{-1}$ above the canopy were used for analysis. Novak et al. (2000) conducted wind tunnel modeling of the experiment by Green et al. (1995) by using artificial Christmas tree branches to model forest canopy elements (LAI = 4.5–0.4, tree density = 333–21 trees per meter squared). Also, Poggi et al. (2004) conducted flume experiments (using rods to model canopy elements) and developed a phenomenological model for varying canopy densities (LAI = 0.51–0.032 $m^2\ m^{-2}$, rod density = 1072–67 rods per meter squared). In each of these studies, normalized turbulent statistics (normalized by either wind speed or friction velocity in the constant shear region above the canopy) showed a systematic behavior with thinning. Normalized wind speed increases, Reynolds shear stress decreases, and the standard deviation of streamwise and vertical velocities increases (Poggi et al. 2004) with thinning.

The aforementioned studies of Green et al. (1995), Novak et al. (2000), and Poggi et al. (2004) focused only on turbulence within and above forest canopies as a function of canopy density. Thistle et al. (2005) examined near-field dispersion as a function of canopy density. They provide evidence that as the canopy is thinned, air motion within the canopy becomes increasingly coupled to air motion above the canopy. Consequently, point source plumes near the ground break apart and become less coherent with lower mean concentrations as the canopy is thinned.

The purpose of this study was to develop a simple numerical technique to guide forest managers in the placement of synthetic semiochemicals being deployed for management of forest insects. Our a priori requirements were that the technique provide three-dimensional predictions of scalar dispersion within a forest canopy while requiring few input parameters and short computational times. To evaluate the predictions, we used data from a unique tracer gas dispersion study that was conducted near Winnfield, Louisiana, where a loblolly pine canopy was successively thinned to an LAI and stem density of 3.71–1.47 $m^2\ m^{-2}$ and 1219–325 stems per hectare, respectively, in four stages (Thistle et al. 2005). Turbulence and scalar dispersion data were collected in each canopy density. In this paper, we review the experimental methods implemented by Thistle et al. (2005), describe the numerical technique used to predict scalar dispersion, and evaluate the numerical results with experimental data. A case study is also presented to show how the numerical technique could be applied by forest managers for a 12-day period.

2. Experimental methods

a. Experimental location and design

The field experiment was conducted at 31°53′23.3″N, 92°50′39.9″W outside of Winnfield on the Winn Ranger District of the Kisatchie National Forest. The site was level with a regularly used, hard dirt road adjacent to the site to the northeast. The total thinned (treatment) area was 1.13 ha. The canopy consisted of an overgrown loblolly pine plantation with canopy tops between 15 and 25 m in height. A dense, hardwood understory had grown in and hardwoods had pushed into the lower canopy so that many of the lower treetops in the overstory were hardwoods. Four tracer releases were conducted in the unthinned (pretreatment) canopy; then the understory was removed and three releases were conducted in the remaining overstory canopy with a basal area of 13 m^2. Three releases were next conducted after the stand was thinned to a basal area of 9.3 m^2, and finally four tests were conducted with the basal area reduced to 6.5 m^2. Each test consisted of 4.5 h of continuous sulfur

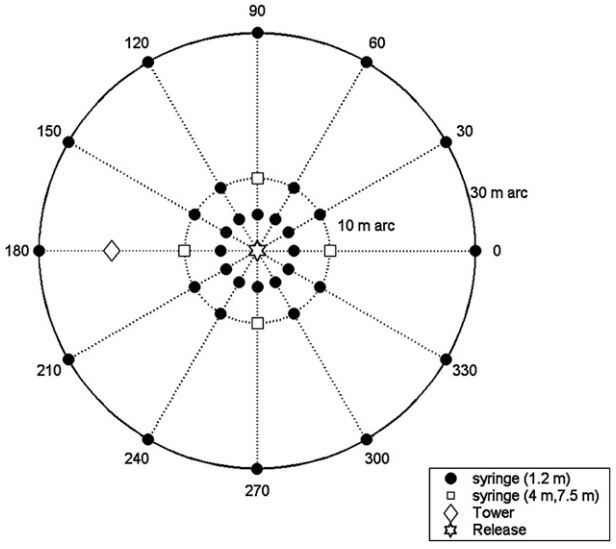

FIG. 1. Experimental design.

hexafluoride (SF_6) tracer gas release and monitoring; the test periods were generally from morning to midday.

The experimental layout is shown in Fig. 1 and is similar to that used by Thistle et al. (2004). The experiment consisted of a variety of turbulence and tracer gas concentration measurements, surrounding a point source of tracer gas. The release location was surrounded with three concentric circles of instruments at 5-, 10-, and 30-m radial distance from the release. At each distance arc, instruments were spaced 30° apart. This design is quite different than traditional cross-streamwise measurements in the sense that the point release was completely surrounded by instruments at different downstream intervals. Thus, downstream concentration data were collected independent of wind direction. This is particularly important inside forest canopies where the wind may be highly variable and decoupled from the winds above the canopy. A tower was erected within the plot at a 20-m distance from the release (to the south) where three levels of turbulence measurements were recorded. Instrumentation used to measure tracer gas concentration, turbulence, and canopy structure is described below.

b. Instrumentation

1) TRACER GAS CONCENTRATION

Tracer gas concentration measurements were made using three types of instruments: syringe samplers (~56 total, 30-min averages), a Trace Gas Automated Profile System (TGAPS) deployed to measure tracer gas vertical profiles (seven levels simultaneously at 5-min averages), and a mobile continuous tracer analyzer that sampled at 1 Hz (one location). During each trial, syringe samplers were deployed at 1.2 m above the ground every 30° on the 5-m arc, and optimally every 15° on the 10- and 30-m arc. In addition, elevated syringe samplers were deployed at 4 and 7.5 m on the 5- and 10-m arcs at 0°, 90°, 180°, and 270°. The TGAPS system was positioned along the 10-m arc at different locations corresponding to wind direction, thus aligning the profiles with the tracer gas plume. Similarly, the continuous tracer gas analyzer was also positioned on the 5- or 10-m arc at different locations to be aligned with the plume. A complete description of the tracer gas experimental layout can be found in Thistle et al. (2005).

2) TURBULENCE

Turbulence measurements were made using three axis, 15-cm pathlength, Vx probe sonic anemometers (ATI, Longmont, Colorado) located at 2.6, 16.6, and 22.9 m on a vertical tower (all heights are above ground level; tower position shown in Fig. 1).

An additional Sx probe ATI sonic anemometer was located at the tracer gas release point, 1.2 m above ground level. Two 7-m meteorological towers were used to provide mean meteorological data, including temperature, humidity (R.M. Young, Model 41372/43372, Traverse City, Michigan), wind speed, and direction (MetOne, Models 5431, 024, 010C, Grants Pass, Oregon). Net radiation (R.E.B.S, Seattle, Washington) was measured at each tower. A RemTech PA0 sodar (Remtech, Inc., Velizy, France) was used in a forest clearing approximately 2 km from the site to monitor the atmosphere above the canopy. The sodar is an acoustic profiler and measures wind speed and direction at 20-m intervals up to a nominal height of 600 m.

3) CANOPY STRUCTURE

Leaf area measurements were made using two methods. The first method utilized a Li-Cor 2000 Plant Canopy Analyzer (PCA; Li-Cor, Inc., Lincoln, Nebraska), which assumes a random distribution of canopy elements and uses a light extinction law to estimate LAI. Because of concerns about the random distribution of elements assumption, we also used a hemispherical photographic technique (HPT) to estimate LAI. Leaf area was measured at 60 points in each canopy density scenario. The PCA gave larger leaf area values in this canopy, yielding LAI values 1.4–1.6 times greater than the HPT. Canopy metrics for the four density scenarios studied are given in Table 1. These values are comparable to values found in the canopy structure literature (Teske and Thistle 2004).

c. Data analysis

The sonic anemometers sampled velocities at 10 Hz. Raw data were stored in half-hour files for postprocessing. Postprocessing consisted of despiking signals greater than five standard deviations and performing a coordinate

TABLE 1. Canopy LAI from the PCA and friction velocity (u_*). Here, LA denotes Louisiana and ba is basal area.

Canopy type	LAI (m^2 m^{-2})	u_* (m s^{-1})
Loblolly pine (LA, unthinned)	3.71	0.38
Loblolly pine (LA, 140 ba)	2.63	0.44
Loblolly pine (LA, 100 ba)	1.98	0.67
Loblolly pine (LA, 70 ba)	1.47	0.7

rotation and tilt correction (Kaimal and Finnigan 1994). Data were filtered based on wind direction to eliminate periods when the turbulence was influenced by the tower. Periods containing more than 10% spikes were eliminated (9.5% of the total data). Each 30-min period was classified by stability classes with the Monin–Obukhov length (L) calculated at the upper anemometer (22.9 m) as

$$L = -\frac{u_*^3}{k\left(\frac{g}{\theta}\right)\overline{w'\theta'}}, \tag{1}$$

where k is the von Kármán constant (0.4), g is the gravitational acceleration (9.81 m s^{-1}), θ is the potential temperature, w is the vertical velocity, and u_* is the friction velocity [$u^* = -\overline{(u'w')}^{0.5}$]. Turbulent statistics were calculated as 30-min means.

Further filtering of data was performed to create a consistent dataset across each thinning. That is, we filtered all data to obtain unstable conditions, wind speeds greater than 1.5 m s^{-1}, and friction velocity greater than 0.35 m s^{-1} to ensure consistent micrometeorological conditions across all thinning treatments. Despite this effort, synoptic-scale conditions changed throughout the experiment. The site was very wet during the dense canopy experiments because of rainfall events, and slowly dried out throughout the thinning.

3. Numerical methods

a. Turbulence model

A suite of numerical techniques exists to predict flow fields within and above forest canopies. One must balance the computational time needed for a particular numerical technique with its desired application. The goal of the present work was to develop a numerical technique that forest managers could reasonably use to guide the placement of synthetic semiochemical sources. Ideally, this numerical technique would be imbedded in a Web-based portal for easy and widespread access. However, this constrains the technique to one that requires limited input data and computational resources.

Consider the data typically available to a forest manager for a given site. Forest managers may have an estimate of the canopy morphology including canopy height, leaf area index, and basal area. From these parameters, one can use canopy structure libraries to calculate leaf area density as a function of height (Teske and Thistle 2004). Canopy effects on momentum and turbulence may then be calculated as a function of height using an assumed drag coefficient. Upper boundary conditions may be calculated from similarity theory, mesoscale models, or measurements. If similarity theory is used, the forest manager must provide an estimated canopy height, zero plane displacement, roughness constant, and friction velocity (or range of friction velocities). Again, this information may be estimated from rules of thumb or a survey of literature produced from similar sites. Lower boundary conditions may be approximated by using wall functions or by assuming negligible gradients. With these input data, the problem is well constrained for numerical purposes.

We now may apply a numerical technique to predict scalar dispersion. To simplify the problem, we assume steady state, an idealized horizontally homogeneous canopy, and a zero pressure gradient. The momentum equation becomes

$$0 = \frac{d}{dz}\left(\nu_t \frac{d\overline{u}}{dz}\right) + S_m, \tag{2}$$

where $\overline{u}$ is the velocity, ν_t is the turbulent viscosity, and S_m is a momentum source term that describes the effect of canopy elements on momentum. Assumptions of steady state, horizontal homogeneity, and a zero pressure gradient are needed for the aforementioned requirements of limiting input data and computational times. Predictions generated when using these assumptions compare well with observations in many forest canopies (Katul et al. 2004). The momentum source term is parameterized as

$$S_m = C_d \alpha |\overline{u}| |\overline{u}_i|, \tag{3}$$

where C_d is a drag coefficient and α is the leaf area density as a function of height. As a starting point, the drag coefficient was assumed to be a constant, and the LAI and canopy height were used to calculate leaf area density as a function of height (Fig. 2) from canopy structure libraries (Teske and Thistle 2004). To close the momentum equation, we must model the turbulent viscosity ν_t. Several models for ν_t have been shown to provide good estimates of plant canopy turbulence. Examples are the mixing length model (Poggi et al. 2004), the one-equation model (Katul et al. 2004), the two-equation model (Katul et al. 2004), and higher-order closure models (Juang et al. 2008). Each model is more complex than the previous one and requires more computational time to generate predictions of the flow field. Each model also provides more information on the flow field than the previous one. For

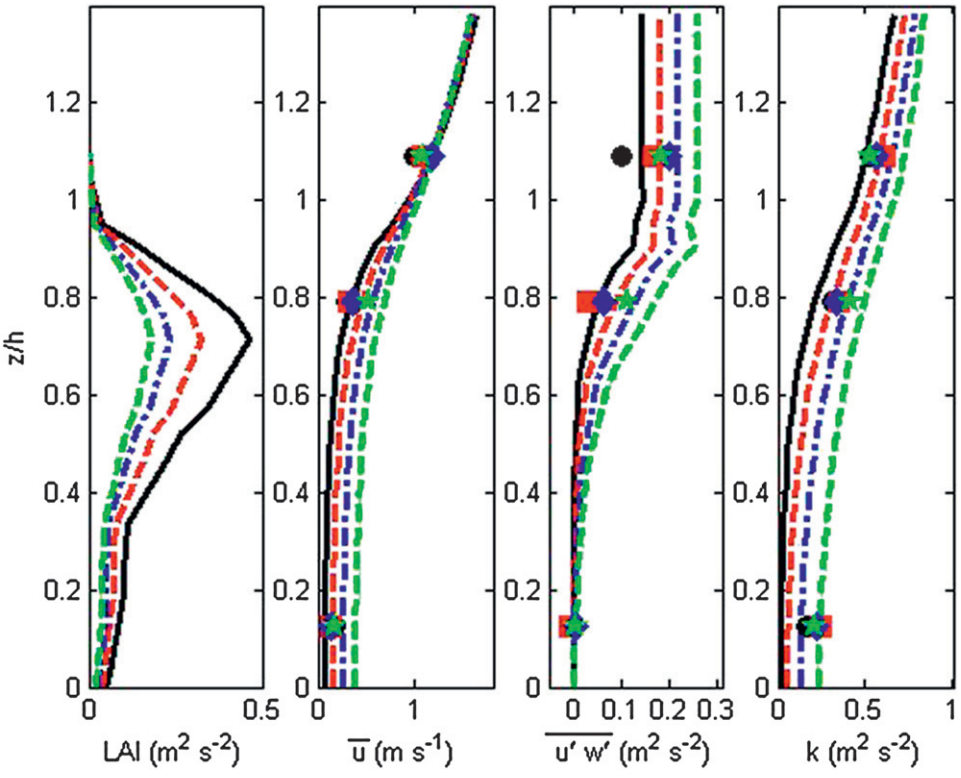

FIG. 2. The (left to right) LAI, wind speed, momentum flux, and turbulent kinetic energy for each canopy density; symbols represent measurements (mean of 30 min corresponds to near-neutral conditions) and lines represent model predictions. symbols and line colors are as follows: black (unthinned canopy), red (first thinning), blue (second thinning), and green (third thinning).

example, the mixing length model describes the flow field with velocity and momentum flux, whereas the two-equation model describes the flow field with velocity, turbulent kinetic energy, and turbulent kinetic energy dissipation rate. Katul et al. (2004) evaluated one- and two-equation models with turbulence data collected in multiple forest canopies and concluded that no additional performance is realized by using a two-equation model for a one-dimensional case. Juang et al. (2008) conclude that one-equation models capture scalar fluxes, but two-equation models perform better than one-equation models by 0%–7%. They also conclude that no additional performance is realized by using higher-order models.

Our goal was to limit computational time and input parameters while providing forest managers with upper and lower bounds of scalar dispersion. We therefore modeled ν_t with a one-equation model, namely the k–l_m turbulence model. Using this approach, one solves one additional equation for turbulent kinetic energy k, and specifies a length scale l_m. The flow field is then described with a velocity, turbulent kinetic energy, and parameterized length scale. Applying the assumptions adopted in the momentum equation, the turbulent kinetic energy equation is

$$0 = \frac{d}{dz}\left(\frac{\nu_t}{\mathrm{Sc}}\frac{dk}{dz}\right) + \nu_t\left(\frac{d\overline{u}}{dz}\right)^2 - \varepsilon + S_k, \tag{4}$$

where $\overline{u}$ is the velocity, k is the turbulent kinetic energy, Sc is the Schmidt number, and S_k represents a canopy source term for turbulent kinetic energy. The dissipation rate ε is modeled as

$$\varepsilon = C_\mu \frac{k^{3/2}}{l_m}, \tag{5}$$

where $C_\mu = 0.09$, the turbulent diffusivity ν_t is

$$\nu_t = C_\mu^{1/4} l_m \sqrt{k}, \tag{6}$$

and the canopy source term for turbulent kinetic energy is (Katul et al. 2004)

$$S_k = C_d \alpha(\beta_p \overline{u}^3 - \beta_d \overline{u} k), \tag{7}$$

where C_d is a drag coefficient, $\alpha$is the leaf area density, β_p and β_d are constants that represent plant elements producing and destroying turbulent kinetic energy, respectively (see Table 2). The length scale l_m physically

TABLE 2. One-equation (k–l_m) model constants.

Constants	
S_c	1.0
C_μ	0.09
C_d	0.3
β_p	0.0
β_d	1.0

represents the length of turbulent eddies that are responsible for transporting momentum and scalars. Since the prediction is inherently an average steady-state solution, l_m represents the transporting eddies on average. In traditional rough wall boundary layers, l_m is parameterized as a function of distance from the wall. In our case, we effectively compute through the roughness (the canopy), thus l_m should use the rough wall form above the canopy. A good approximation of l_m above the canopy (in the convective boundary layer) is (Kaimal and Finnigan 1994)

$$l_m = k_v(z - d), \tag{8}$$

where k_v is the von Kármán constant and d is the displacement height [$d = (2/3)h$ for dense canopies]. Within the canopy, l_m is not well resolved. Recent experiments have shown that l_m is constant within the canopy, at least for dense canopies (Katul et al. 2004). Poggi et al. (2004) suggest that near the ground, l_m is a function of the diameter of rods (rods because the study was conducted within a wind tunnel). We adopted the assumption that l_m is constant within the canopy for dense canopies; however, we propose to model l_m within the canopy to include canopy density effects as

$$l_m = C(ah), \tag{9}$$

where $C = 1$ for $\mathrm{LAI} \geq \mathrm{LAI}_{\mathrm{dense}}$ and $C = \mathrm{LAI}_{\mathrm{dense}}/\mathrm{LAI}$ for $1 \leq \mathrm{LAI} < \mathrm{LAI}_{\mathrm{dense}}$. This form ensures that as the canopy is thinned (becomes less dense) the length scale increases, which is in agreement with the formulation in Poggi et al. (2004). However, for $\mathrm{LAI} > 1$ we do not specify a length scale parameterization. In this case the boundary layer length scale parameterization may be more important. Also, we caution that this parameterization is well suited for forest canopies, and smaller plant canopies were not considered in this study. We selected the LAI of the unthinned canopy (3.71) as $\mathrm{LAI}_{\mathrm{dense}}$, and tested this parameterization against a constant length scale for all canopies.

b. Three-dimensional scalar dispersion model

Assuming steady-state, horizontal homogeneity, and negligible molecular diffusion, the three-dimensional time-averaged turbulent diffusion equation for a scalar is

$$\overline{u}\frac{\partial\overline{\phi}}{\partial x} = -\left(\frac{\partial\overline{\phi' u'}}{\partial x} + \frac{\partial\overline{\phi' v'}}{\partial y} + \frac{\partial\overline{\phi' w'}}{\partial z}\right) + S_\phi, \tag{10}$$

where $\overline{u}$ is the average horizontal wind speed, $\overline{\phi}$ is the average scalar concentration, S_ϕ is a source term, and the prime denotes a departure from the mean. Closure for Eq. (10) was achieved using the Boussinesq approximation (Wilcox 1993) where

$$\overline{\phi' u_i'} = -\frac{\nu_t}{\sigma_t}\frac{\partial\overline{\phi}}{\partial x_i}. \tag{11}$$

Recall the turbulent viscosity, ν_t, is calculated with Eq. (6), and $\sigma_t = 0.9$ is the turbulent Schmidt number. Substituting Eq. (11) into Eq. (10) yields

$$\overline{u}\frac{\partial\overline{\phi}}{\partial x} = \frac{\partial}{\partial x_i}\left(\frac{\nu_t}{\sigma_t}\frac{\partial\overline{\phi}}{\partial x_i}\right) + S_\phi. \tag{12}$$

Note that the turbulent diffusivity is the same in the horizontal directions as the vertical direction. This assumption is fundamentally incorrect because scalars are not transported the same in the horizontal and vertical directions. The assumptions needed for one-dimensional, horizontally homogenous flow field predictions limit us from calculating horizontal diffusivities. This is true for one-dimensional mixing length, as well as one- and two-equation models. Several alternatives exist, such as setting the horizontal dispersion as a function of the vertical dispersion, using plume meander equations, or solving separate transport equations for horizontal fluxes. To stay consistent with developing a simple model, we elect to set the horizontal diffusivity as a function of the vertical diffusivity. As a first step we set these values equal; however, this resulted in an overprediction of downstream concentration. To improve this parameterization, we set the horizontal diffusivity to be twice that of the vertical diffusivity, which is consistent with velocity length scales across a range of canopies (Finnigan 2000).

c. Domain and boundary conditions

The momentum and turbulent kinetic energy equations were solved over a one-dimensional domain extending 40 m from the ground with 1-m cell resolution. The same vertical dimension was used to solve for scalar concentration with horizontal dimensions of 100 m in each direction.

We used zero gradient boundary conditions for wind speed and turbulent kinetic energy at the lower boundary for all canopies. These boundary conditions are valid

for forest canopies because the majority of the momentum is absorbed by canopy elements resulting in negligible Reynolds stress at the wall (Yi 2008). Upper wind speed and turbulent kinetic energy of 2.0 m s^{-1} and 0.9 m^2 s^{-2}, respectively, were specified for all canopies. These values were obtained from the filtered observational dataset.

A fully reflecting boundary condition (zero gradient) was used at the lower boundary for scalar concentration. Zero concentration values were applied at all other boundaries, since the domain size, release location, and receptor locations were sufficiently far away from the boundaries that the boundaries did not affect the local concentration.

4. Results and discussion

a. Turbulence statistics

Measurement heights are referred to as the upper ($z/h = 1.14$), middle ($z/h = 0.83$), and lower ($z/h = 0.13$) anemometers ($h = 20$ m). Profiles of observed and predicted wind speed, momentum flux, and turbulent kinetic energy are shown in Fig. 2. Wind speed, momentum flux, and turbulent kinetic energy slightly varied with canopy density (due to filtering) so that constant micrometeorological conditions for all canopy densities were ensured. The observed wind speed, momentum flux, and turbulent kinetic energy increased with thinning at the middle and upper anemometer. At the lower anemometer, observed wind speed and momentum flux did not increase with thinning, while turbulent kinetic energy did increase with thinning. Predicted wind speed increased with thinning and compares well with observations. A goodness of fit (R^2) was calculated for each variable as

$$R^2 = 1 - \sum_i \frac{(P_i - O_i)^2}{O_i}, \tag{13}$$

where P_i is the predicted value, O_i is the observed value, and i is the index for measurement height. Wind speed was predicted well for the unthinned and first thinning canopies ($R^2 > 0.90$), but overpredicted at the lower anemometer for the second ($R^2 = 0.74$) and third thinning ($R^2 = 0.68$) canopies. Momentum flux was predicted well at each height for all canopies ($R^2 > 0.90$). Turbulent kinetic energy was underpredicted for the unthinned ($R^2 = 0.83$) and first thinning ($R^2 = 0.84$) canopy, predicted well for the second thinning ($R^2 = 0.94$), and overpredicted for the third thinning ($R^2 = 0.90$) canopy.

The differences between predictions and observations may be attributed to uncertainties in the $k - l_m$ turbulence model, such as the length scale, boundary conditions, and canopy source terms. The k–ε closure scheme eliminates the specification of a length scale; however, the additional complexity may not result in overall improved performance because of uncertainties in model constants and canopy source terms for the dissipation rate (Katul et al. 2004). Our choice of zero gradient lower boundary conditions requires that all momentum be absorbed by the plant canopy elements. This may be invalid for sparse canopies, however, observed momentum flux suggests that it is valid for the present range of canopy densities (LAI = 3.71–1.47 m^2 m^{-2}). There are many constants in the canopy source term parameterization. We performed a sensitivity analysis on model parameters to assess and improve model performance. Wind speed, momentum flux, and turbulent kinetic energy were evaluated to determine the appropriate constants for the present canopy (data not shown). The source term from Katul et al. (2004) and associated constants do, however, remain a source of uncertainty in applying this model to other canopies without conducting a sensitivity analysis.

b. Scalar dispersion

Scalar concentration predictions were evaluated in three ways: 1) the ability of the model to capture general trends in maximum downstream tracer gas concentrations versus canopy density, 2) the ability of the model to predict vertical concentration gradients at a distance 10 m from the gas release point, and 3) the ability of the model to predict cross-streamwise concentration gradients at each arc (5, 10, and 30 m downstream). In all of the aforementioned tests, concentration data were filtered to match the aforementioned turbulence data filtering to ensure consistent micrometeorological conditions for all canopy densities.

To evaluate the model performance for general trends of scalar dispersion as a function of canopy density, we calculated aggregate means of the maximum concentration at each arc for each thinning. These data were compared with the predicted centerline concentration at each arc for each canopy density (Fig. 3). Maximum normalized concentrations decreased with thinning at all arcs, and were well captured by the model as shown in a 1:1plot (Fig. 4).

To test the parameterization for the length scale, we ran the model with a constant length scale for all canopy densities (Fig. 3). This parameterization overpredicted scalar concentration at all arcs for the less dense canopies. Thus our parameterization of the length scale as a function of LAI seems appropriate for scalar dispersion in this canopy.

Next, we used observations of vertical concentration gradients at a distance of 10 m from the source to evaluate the model in terms of vertical scalar dispersion.

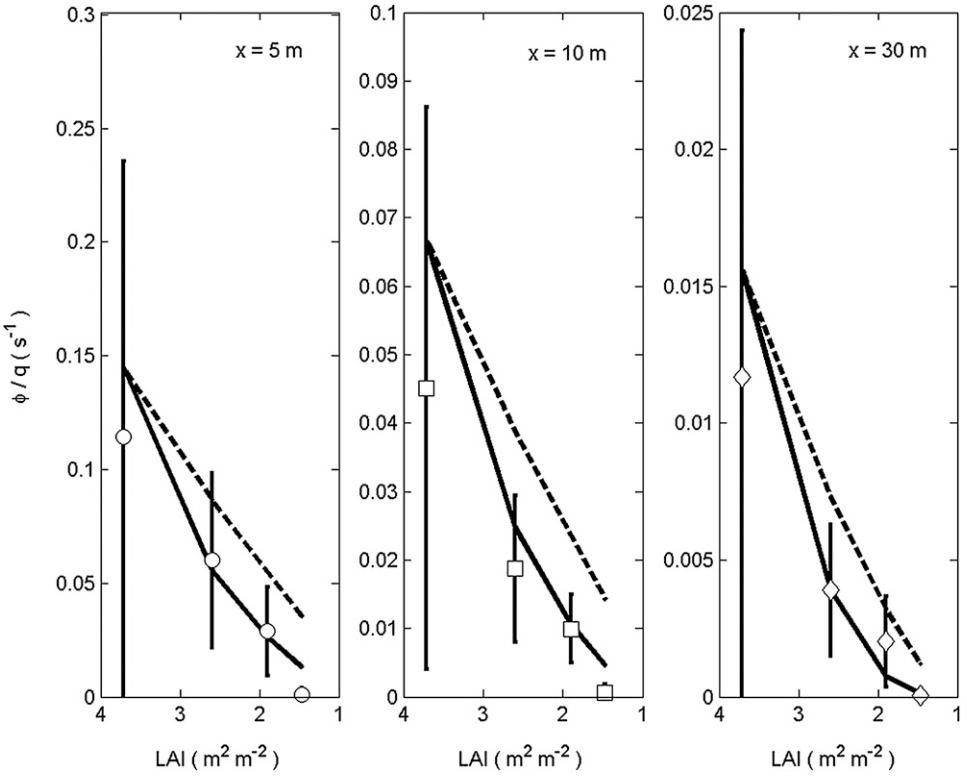

FIG. 3. Observed max and $\pm 1\ \sigma$ of max arc normalized concentration vs LAI for each arc (symbols). Predicted max arc normalized concentration for l_m = constant for all canopies (dashed line), and $l_m = f(\text{LAI})$ (solid line).

Predicted centerline vertical concentration gradients were evaluated with mean concentrations from the elevated syringe samplers (4 and 7.5 m above the ground) and the TGAPS system for each thinning (Fig. 5). The vertical concentration gradient is slightly overpredicted for each canopy except the thinnest canopy (LAI = 1.46). However, this may be a result of an inappropriate comparison. That is, the model data are true centerline concentrations, but each measurement is not a centerline concentration because of plume meander. The observed concentration will either be at, or below, the centerline concentration, resulting in a lower mean concentration. Thus, we expect the centerline model concentration to overpredict observations.

To evaluate model performance for predicting horizontal gradients of concentration at each arc, we compared those model cell locations that corresponded with the polar coordinates of the arc measurements with the measured scalar concentration at each arc for each trial. Mean and one standard deviation of SF_6 concentrations for one trial from each thinning are shown in Figs. 6–9. The arc location of the observed concentration was adjusted to coincide with the location of the centerline predicted concentration. This is identical to adjusting the wind direction in the model to correspond with observed wind direction.

Individual trial period data show key characteristics of plume dispersion within a canopy and the effect of measuring concentration in concentric rings versus lateral

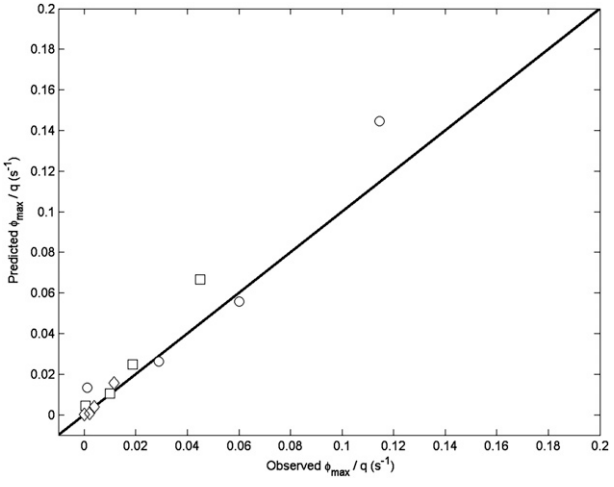

FIG. 4. Mean of max observed normalized concentrations vs max predicted normalized concentration at the 5- (circles), 10- (squares), and 30-m (diamonds) arcs.

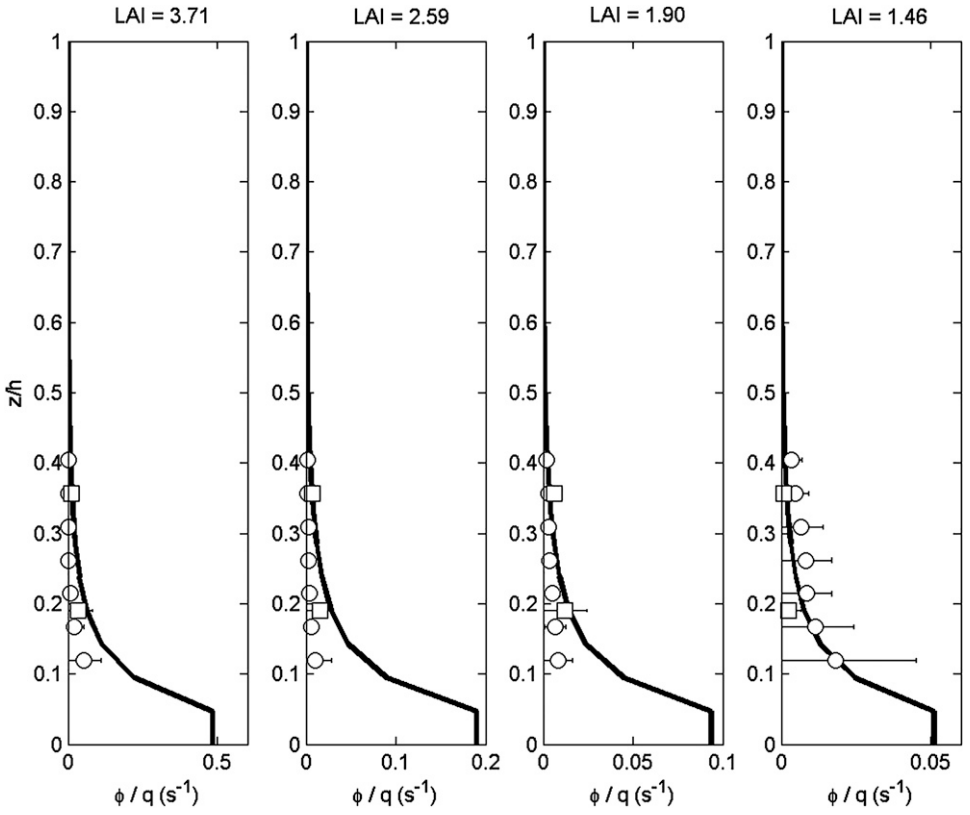

FIG. 5. Predicted (solid line) and observed (symbols) vertical profiles of mean normalized concentration at the 10-m arc. Observational data are from two instruments: the TGAPS system (circles; varying averaging times depending on deployment $\pm 1\ \sigma$) and elevated syringe samplers (squares; one 4.5-h period $\pm 1\ \sigma$): (left to right) LAI from 3.71 to 1.46.

lines. Lateral line measurements show clear plumes with near-zero concentrations at the tails and high standard deviations of concentrations near the tails. However, measuring scalar concentrations on concentric circles revealed significant normalized concentrations at all positions on each arc for each trial, with the exception of the 30-m arc following the third thinning canopy. This is evidence that the plume is dispersed in all directions from the release, independent of the mean wind direction. This is not surprising because of low wind velocities observed within the canopy and the highly variable wind direction within the canopy. This feature is captured well by the model. Second, contrary to lateral concentration observations, the largest standard deviations are located at the point of maximum concentration, not at the tails of the distribution. This suggests that very intermittent high concentrations of tracer gas dominate the 30-min average at the peak concentration. Finally, plumes are clearly identifiable on each arc in the unthinned and first thinning canopy plots, and are harder to identify in the second and third thinning plots. This is evidence that as the canopy is thinned, plumes become less coherent because of increasing intermittency within the canopy.

Strand et al. (2009) used a Lagrangian puff model to predict tracer gas dispersion in a lodgepole pine canopy (stem density = 1521 stems per hectare, canopy height = 30 m, LAI = 2.5) and a ponderosa pine canopy (stem density = 389 stems per hectare, canopy height = 35 m, LAI = 3.3). Their model used 1-Hz sonic anemometer winds to drive the advection of each puff, and dispersion theory to calculate puff growth. Predictions were compared with experimental data from an identical tracer gas dispersion experimental design as described in this study. Average fraction errors for each canopy at each arc were below 50%. Fractional errors were larger at the 30-m arc, and larger for the less dense canopy (ponderosa pine). Our model had similar performance trends; that is, our errors were larger for the less dense canopy (Table 3). Our model had slightly lower magnitudes of fractional error for all canopies except the third thinning as compared with Strand et al. (2009). However, our model had larger fraction errors for the third thinning canopy as compared to Strand et al. (2009).

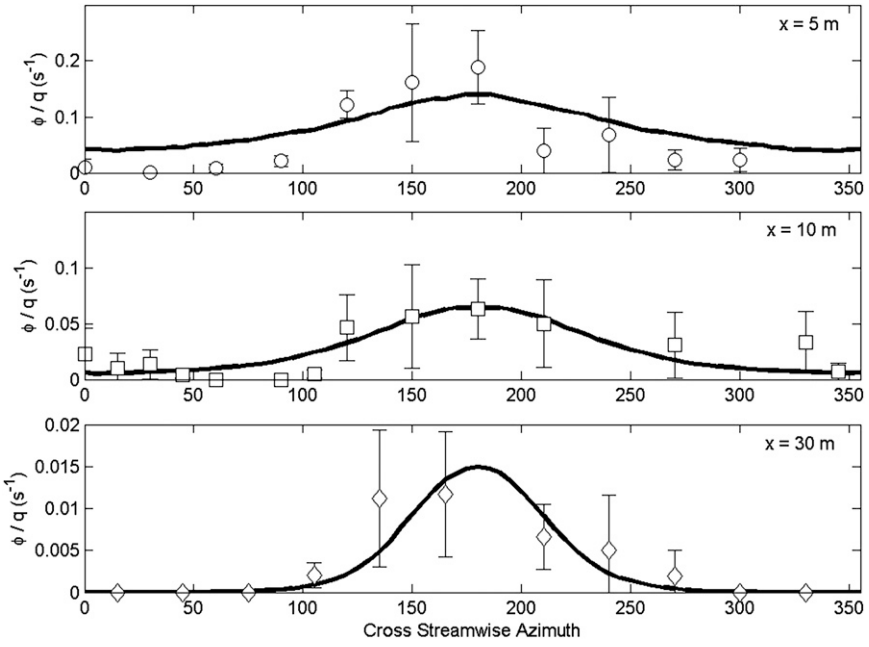

FIG. 6. Unthinned canopy (LAI = 3.71 m^2 m^{-2}): cross-streamwise predicted (solid line) and observed (symbols) mean normalized concentration at each arc: x = (top) 5, (middle) 10, and (bottom) 30 m. Observations represent one 4.5-h period ($\pm 1\ \sigma$).

The simple k–l_m turbulence model generally predicted normalized concentrations for individual trials, and aggregate maximum normalized concentrations, to within $\pm 1\ \sigma$. Considering the simplicity of the model and the uncertainty in the length scale, boundary conditions, and source terms, we consider model performance to be good. Predictions also captured changes in trends of normalized concentrations associated with thinning. The one-dimensional turbulence model provided vertical diffusivities that were used to drive both vertical and

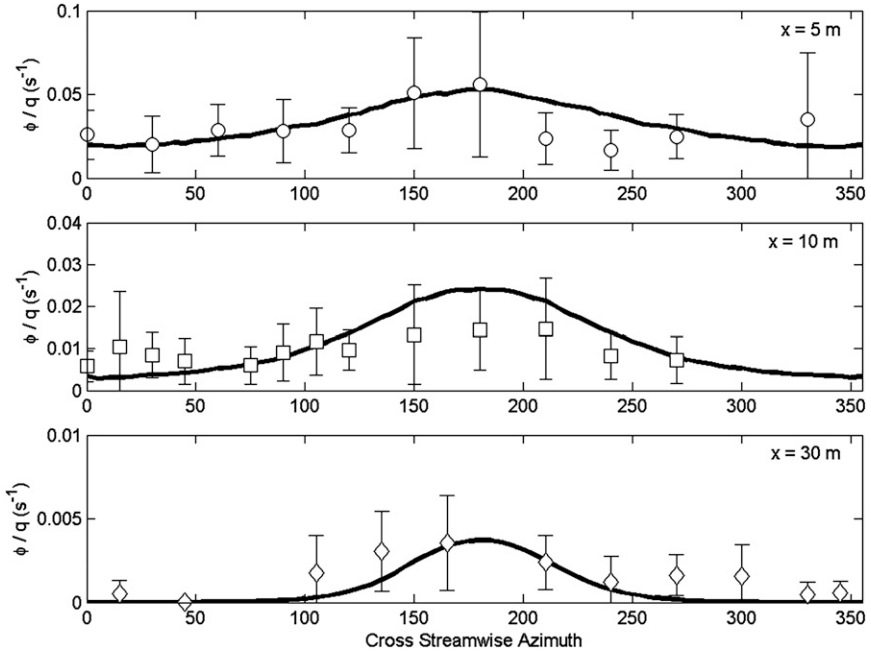

FIG. 7. As in Fig. 6, but for first thinning (understory removal; LAI = 2.63 m^2 m^{-2}).

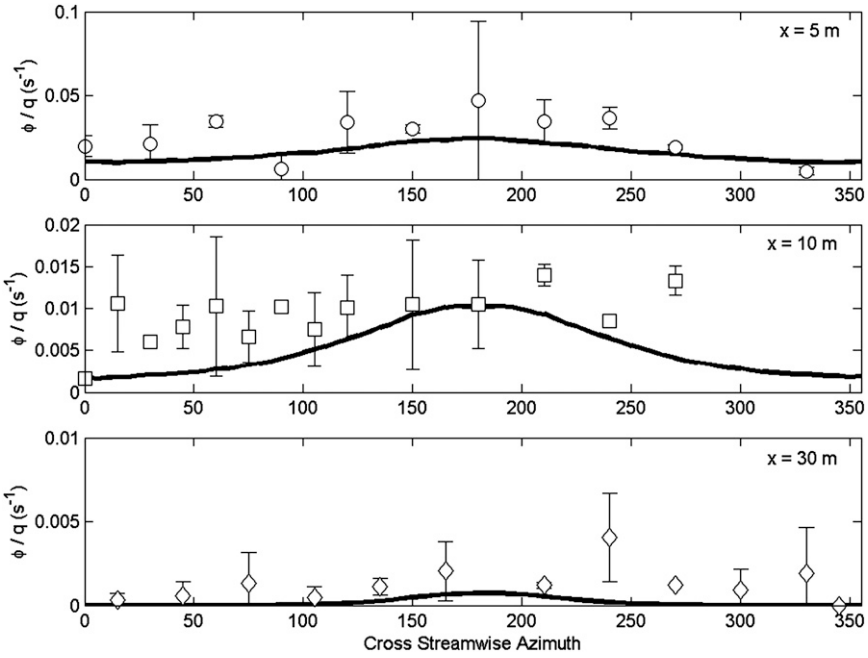

FIG. 8. As in Fig. 6, but for second thinning (LAI = 1.98 m^2 m^{-2}).

horizontal dispersion. This assumption is strictly invalid; however, horizontal dispersion was shown to compare well with observations by comparing trial data. Therefore, as a first step in providing forest managers with upper and lower bounds of scalar dispersion, this assumption may be adequate. The short computational time and low degree of parameterization make this model well suited for online applications by forest managers, as long as there is an understanding of input uncertainties and associated errors.

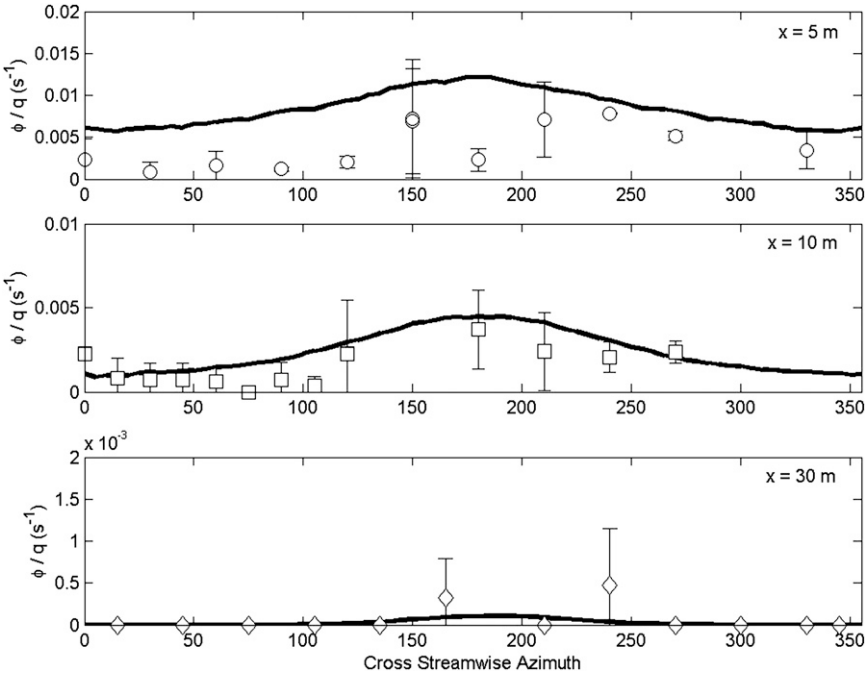

FIG. 9. As in Fig. 6, but for third thinning (LAI = 1.47 m^2 m^{-2}).

TABLE 3. Fractional error in mean max concentration (%) at each arc (m) for each canopy.

Canopy/arc	5	10	30
Loblolly pine (LA, unthinned)	23	39	29
Loblolly pine (LA, 140 ba)	8	28	1
Loblolly pine (LA, 100 ba)	10	9	90
Loblolly pine (LA, 70 ba)	167	157	86

c. Application study

One advantage of using a simple numerical technique to predict scalar dispersion is its short computational time. The model presented here runs in a few minutes, and thus is well suited for a Web-based portal that could be easily made available to forest managers. To explore this application, consider data available to forest managers: these data may include estimates of leaf area index and canopy height regardless of direct measurements. With these data, managers can use the tables provided by Teske and Thistle (2004) to calculate a vertical profile of LAI, which may then be used to calculate the source–sink profiles for momentum and turbulence. Upper boundary conditions can be determined from measurements or mesoscale atmospheric models and similarity theory. If similarity theory is used, the forest manager must provide an estimated canopy height, zero plane displacement, roughness constant, and friction velocity (or range of friction velocities). This information may be estimated from rules of thumb or literature. Friction velocities may be approximated rather crudely, and the model can be run in a sensitivity mode. For example, assume the forest manager has an estimate of wind speed from either measurements or a mesoscale model. For a forest canopy similar to this study, the manager may assume a range of friction velocities between 0.25 to 0.75 $m^2\ m^{-2}$. Using similarity theory equations, the manager can then calculate upper turbulent kinetic energy. With these limited data, the forest manager may now use the model. This application could be for one period or multiple periods, as well as sensitivity studies.

To test a multiple period application, we ran the model for 12 days using measured winds from a sodar. This example illustrates how resource managers may use the technique to predict scalar concentrations for multiple days and use the results as upper and lower bounds to guide them in the placement of synthetic semiochemical sources. For this example, we set the canopy density to the unthinned value (LAI = 3.71 $m^2\ m^{-2}$). Twelve days of sodar winds at 40 m (height from ground) were used for the upper-velocity boundary conditions. Similarity theory was used to calculate the friction velocity and the upper boundary condition of turbulent kinetic energy.

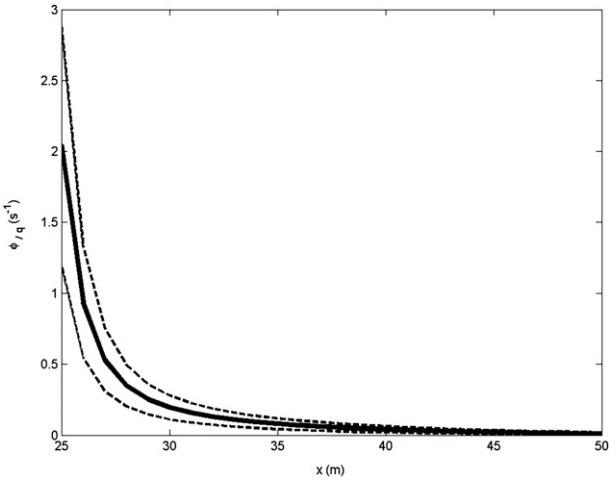

FIG. 10. Predicted mean (solid line) and $\pm 1\ \sigma$ (dashed lines) of streamwise normalized concentration for a 12-day period.

Model output consists of ensemble means ($\pm 1\sigma$) of streamwise, cross-streamwise, and vertical scalar concentration profiles, which are shown in Figs. 10–12. These plots may be used to determine semiochemical source placement and the strength needed for a given coverage area. For example, if a coverage of 0.01 (s^{-1}) normalized concentration was desired, traps would be placed approximately 25 m apart in the streamwise direction, 30 m apart in the cross-streamwise direction, and would extend from the surface to near $0.6h_c$ (h_c = canopy height) vertically.

With its short computational time and limited input data requirement (canopy height, LAI, and wind speed), this model is ideal for use in a Web-based portal. We caution that the model has only been evaluated for a loblolly pine canopy with a constant height and slightly unstable conditions. This is because we are focused on pheromone dispersion for bark beetles, which are most active during slightly unstable conditions.

5. Conclusions

We presented experimental turbulence and scalar dispersion results from a unique tracer gas dispersion experiment. In the experiment, a loblolly pine canopy was successively thinned to an LAI and stem density of 3.71–1.47 $m^2\ m^{-2}$ and 1219–325 stems per hectare, respectively, in four stages. Turbulence and scalar concentration data were collected in each stage of thinning. A k–l_m turbulence model was used to predict flow fields for use with a three-dimensional scalar dispersion model.

Generally, thinning resulted in an increase in wind speed and turbulence within the canopy. This caused a reduction in plume meander and an increase in plume dilution, resulting in lower mean concentrations of

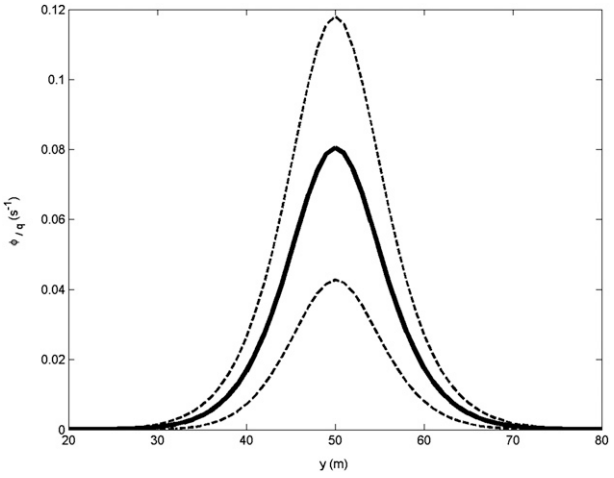

FIG. 11. As in Fig. 10, but for cross-streamwise normalized concentration.

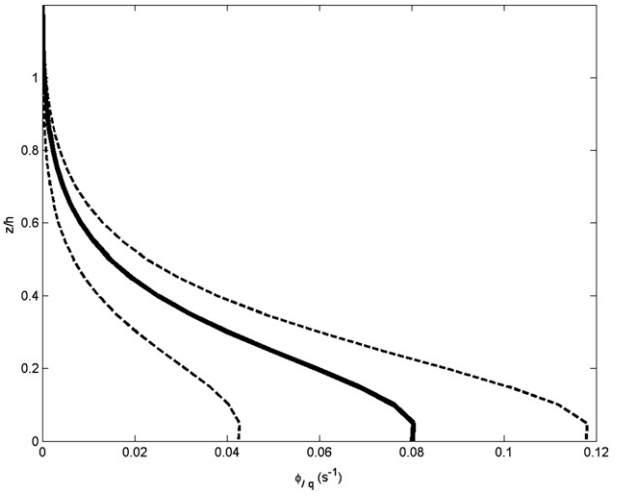

FIG. 12. As in Fig. 10, but for vertical normalized concentration.

tracer gas within the canopy. Predictions were compared with experimental data and showed good agreement for wind speed and turbulent kinetic energy. Predicted normalized concentrations from individual trials and aggregate means compared well with observations.

Using concentric circles centered on the tracer release location versus lateral downstream lines as measuring receptors revealed unique characteristics of in-canopy dispersion. First, upstream dispersion was observed on the 5-, 10-, and 30-m arcs with the exception of the 30-m arc following the third thinning. Second, the location of the largest standard deviations corresponded with the location of maximum concentration, which is contrary to lateral line measurements. Finally, a clear plume was identifiable for the dense canopies but not for the sparse canopies.

Predicted fractional errors were comparable to those of Strand et al. (2009). The simple Eulerian modeling approach presented here has a short computational time and requires few input parameters as compared to the model of Strand et al. (2009). Thus, the model is ideal for Web-based use by forest managers. To verify this applicability, we predicted scalar dispersion for a 12-day period using sodar measurements as a driving force. Ensemble mean scalar concentration profiles, based on the 12-day period, were presented. These results are an example of predictions that forest managers may use as upper and lower bounds to guide the placement of semiochemical sources.

Acknowledgments. We acknowledge the work of Anna Carter and Kyle Heitkamp (Montana Technical University), Theo Leonard and Rachael Allwine (Washington State University), Scott Gilmour, Wes Throop, Jim Kautz, and Mike Huey (USDA Forest Service, MTDC, Missoula, MT), and R. Arnold and S. Walters (USDA Forest Service, SRS, Pineville, LA) in field sampling and organization as well as Denise Binion for layout support. We thank Robert Howell, Frank Yerby, and Jim Meeker for support and local arrangements, as well as the remaining staff of the Winn Ranger District of the Kisatchie National Forest. This work was supported by USDA-FS-FHTET-FHP-TD. 00.M03, USDA-FS-SRS-RWU-4501, and USDA-FS-Region 8, Forest Health Protection.

REFERENCES

Allen, L. H., 1968: Turbulence and wind speed spectra within a Japanese larch plantation. *J. Appl. Meteor.,* **7,** 73–78.

Baldocchi, D. D., and B. A. Hutchinson, 1987: Turbulence in an almond orchard: Vertical variations in turbulent statistics. *Bound.-Layer Meteor.,* **40,** 127–146.

——, and T. P. Meyers, 1988: Turbulence structure in a deciduous forest. *Bound.-Layer Meteor.,* **43,** 345–364.

Finnigan, J. J., 2000: Turbulence in plant canopies. *Annu. Rev. Fluid Mech.,* **32,** 519–571.

Green, S. R., J. Grace, and N. J. Hutchings, 1995: Observations of turbulence air flow in three stands of Sitka spruce. *Agric. For. Meteor.,* **74,** 205–225.

Juang, J., G. G. Katul, M. B. Siqueira, P. C. Stoy, and H. R. McCarthy, 2008: Investigating a hierarchy of Eulerian closure models for scalar transfer inside forested canopies. *Bound.-Layer Meteor.,* **128,** 1–32.

Kaimal, J. C., and J. J. Finnigan, 1994: *Atmospheric Boundary Layer Flows: Their Structure and Measurement*. Oxford University Press, 289 pp.

Katul, G. G., L. Mahrt, D. Poggi, and C. Sanz, 2004: One- and two-equation models for canopy turbulence. *Bound.-Layer Meteor.,* **81,** 81–109.

Lee, X., 2000: Air motion within and above forest vegetation in non-ideal conditions. *For. Ecol. Manage.,* **135,** 3–18.

Novak, M. D., J. S. Warland, A. L. Orchansky, R. Ketler, and S. Green, 2000: Wind tunnel and field measurements of turbulent flow in forests. Part I: Uniformly thinned stands. *Bound.-Layer Meteor.,* **95,** 457–495.

Nowak, J., C. Asaro, K. Klepzig, and R. Billings, 2008: Southern Pine Beetle prevention initiative: Working for healthier forests. *J. For.,* **106,** 261–267.

Poggi, D., A. Porporato, L. Ridolfi, J. D. Albertson, and G. G. Katul, 2004: The effect of vegetation density on canopy sub-layer turbulence. *Bound.-Layer Meteor.,* **111,** 565–587.

Raupach, M. R., J. J. Finnigan, and Y. Brunet, 1996: Coherent eddies and turbulence in vegetation canopies: The mixing layer analogy. *Bound.-Layer Meteor.,* **78,** 351–382.

Strand, T., B. Lamb, H. Thistle, E. Allwine, and H. Peterson, 2009: A simple model for simulation of insect pheromone dispersion within forest canopies. *Ecol. Modell.,* **220,** 640–656.

Teske, M. E., and H. W. Thistle, 2004: A library of forest canopy structure for use in interception modeling. *For. Ecol. Manage.,* **198,** 341–350.

Thistle, H. W., H. G. Peterson, G. Allwine, B. Lamb, T. Strand, E. Holsten, and P. Shea, 2004: Surrogate pheromone plumes in three forest trunk spaces: Composite statistics and case studies. *For. Sci.,* **50,** 610–625.

——, ——, ——, S. L. Edburg, B. K. Lamb, and B. Strom, 2005: Pheromone movement in four stand thinning scenarios: High frequency plume observations. ASAE Tec. Paper 051002, American Society of Agricultural Engineers, St. Joseph, MI, 11 pp.

USDA Forest Service, 2004: Forest insect and disease conditions in the United States 2003. 53rd Annual Rep., Forest Health Protection Office, Washington, DC, 142 pp. [Available online at http://permanent.access.gpo.gov/lps40040/LPS40040/www.fs.fed.us/foresthealth/publications/ConditionsReport_03_final.pdf.]

Wilcox, D. C., 1993: *Turbulence Modeling for CFD*. DCW Industries, 537 pp.

Yi, C., 2008: Momentum transfer within canopies. *J. Appl. Meteor. Climatol.,* **47,** 262–275.